Electronic Supplementary Material (ESI) for Materials Chemistry Frontiers.

Pyrazoloanthrone-Functionalized Fluorescent Copolymer for the Detection and Rapid analysis of Nitroaromatics

S. Saravanan,[a,#] Rafiq Ahmad,[a,#] S. Kasthuri,[a] Kunal Pal,[b] S. Raviteja,[c] P. Nagaraaj,[d] Richard Hoogenboom,[e,*] Venkatramaiah Nutalapati,[a,*] and Samarendra Maji [a,*]

[a]Department of Chemistry, Faculty of Engineering and Technology, SRM Institute of Science and Technology (SRMIST), Kattankulathur, Tamil Nadu- 603203, India.

[b]Department of Biotechnology and Medical Engineering, National Institute of Technology, Rourkela- 769008, India.

[c]Solid State and Structural Chemistry Unit (SSCU), Indian Institute of Science (IISc), Bangalore 560012, India

[d]Department of Chemistry, College of Engineering Guindy, Anna University, Chennai-600025, India.

[e]Supramolecular Chemistry Group; Centre of Macromolecular Chemistry, Department of Organic and Macromolecular Chemistry; Ghent University; Krijgslaan 281 S4; Ghent, Belgium.

To whom correspondence should be addressed

Dr. Venkatramaiah Nutalapati, **E-mail: nvenkat83@gmail.com*

Dr. Samarendra Maji, **E-mail: samarenr@srmist.edu.in*

Prof. Richard Hoogenboom, **E-mail: richard.hoogenboom@ugent.be*

[#] These authors contributed equally to this work.

Table of Contents

1. Characterization

^{1}H-NMR spectrum of SP-OH is shown in (**Fig. S1**). Two new signals appear at 4.60 and 4.24 ppm with coupling constants of 4.8 Hz and 4.75 Hz respectively are characteristics of two methylene groups and one broad signal at 3.31 ppm characteristics of hydroxyl group confirming that the hydrazine ethanol has got condensed with 1-chloroanthraquinone. ^{13}C-NMR signal at 183.65 ppm confirms that SP-OH having one carbonyl functionality (**Fig. S2**). ESI-MS result of molecular ion peak m/z 265.09 $[M+H]^+$ supports the formation of the desired compound (**Fig. S3**). ^{1}H-NMR of SP-COOH showed two different types of methylene environments due to the incorporation of succinic anhydride *via* ring-opening with the SP-OH compound. Methylene groups which are attached to the less acidic environment and towards the aromatic group are more de-shielded. These methylene protons give two signals between 4.89-4.53 ppm in the ^{1}H NMR spectrum (**Fig. S4**) measured in DMSO-d_6 and each signal got split into three peaks and appears as two triplets due to the coupling by the nearby two protons with the coupling constants of 4.9 Hz and 5.05 Hz respectively. The other two methylene groups appear at 2.34-2.37 ppm due to the comparatively shielding environment.

^{13}C-NMR spectrum showed three different types of carbonyl signals in the spectrum and supports the structure of SP-COOH (**Fig. S5**). LC-MS result of molecular ion peak m/z 363.05 $[M-H]^-$ supports the formation of the desired compound (**Fig. S6**). FT-IR spectrum of SP-OH showed the stretching vibrations in the regions 3418 cm^{-1} due to O-H stretching, 3100-2850 cm^{-1} assigned to aromatic and aliphatic C-H stretching, 1642 cm^{-1} due to carbonyl C=O stretching and 1496 cm^{-1} assigned to aromatic C=C stretching vibrations and supports the formation of SP-OH compound. IR spectra of SP-COOH compound is shown in **Fig. S7**. The compound showed the stretching bands at 1635, 1660, and 1733 cm^{-1} in characteristics of ketone, acid, and esters functional group present in the compound whereas, 1500 cm^{-1} due to the C=C stretching vibrations of the aromatic ring. From the **Fig. S7**, it is also visible that the intensity of O-H stretching vibration at 3425 cm^{-1} has got diminished due to the linkage of succinic anhydride with the hydroxyl end group of SP-OH. ^{1}H-NMR spectrum of $mPEG_{48}$-*b*-PHEA is shown in (**Fig. S9**). The broadening of the signal was observed between 2.7-1.5 ppm due to the formation of the macromolecular chain. Two methylene groups appear between 4.5-3.5 ppm. Molecular weight could not determine due to the overlapping of peaks. For future calculations, we have considered the molecular weight calculated *via* GC method. Moreover, IR spectrum of the block copolymer exhibited characteristic O-H stretching vibration at

3435 cm^{-1} of HEA repeat units, 2890 cm^{-1} due to aliphatic C-H stretching vibrations, 1736 characteristics of C=O stretching vibrations of ester functionality present in the block copolymer (**Fig. S10**).

Later, SP-COOH was conjugated via DCC coupling reaction of COOH of SP-COOH molecule (anthrapyrazolone analogue) and the O-H functionality of HEA present in the block (co)polymer $mPEG_{48}$-*b*-PHEA (**Scheme 1**) in presence of DMAP. ^{1}H-NMR spectrum of the ($mPEG_{48}$-*b*-PHEA)-SP is shown in **Fig. S11**. ^{1}H-NMR signals appear between 8.5 and 7.5 ppm are characteristics of fluorophore molecules that are attached to the block (co)polymer $mPEG_{48}$-*b*-PHEA. Moreover, two triplets appear at 4.70 and 4.56 ppm is attributed to the aliphatic two methylene protons that are connected to the side of aromatic unit. However, due to overlapping signals in the ^{1}H NMR spectrum of ($mPEG_{48}$-*b*-PHEA)-SP we could not determine the degree of functionalization. IR spectra also support the formation of fluorophore-conjugated block (co)polymer as all the characteristics stretching vibration are available in the IR spectrum (**Fig. S10**).

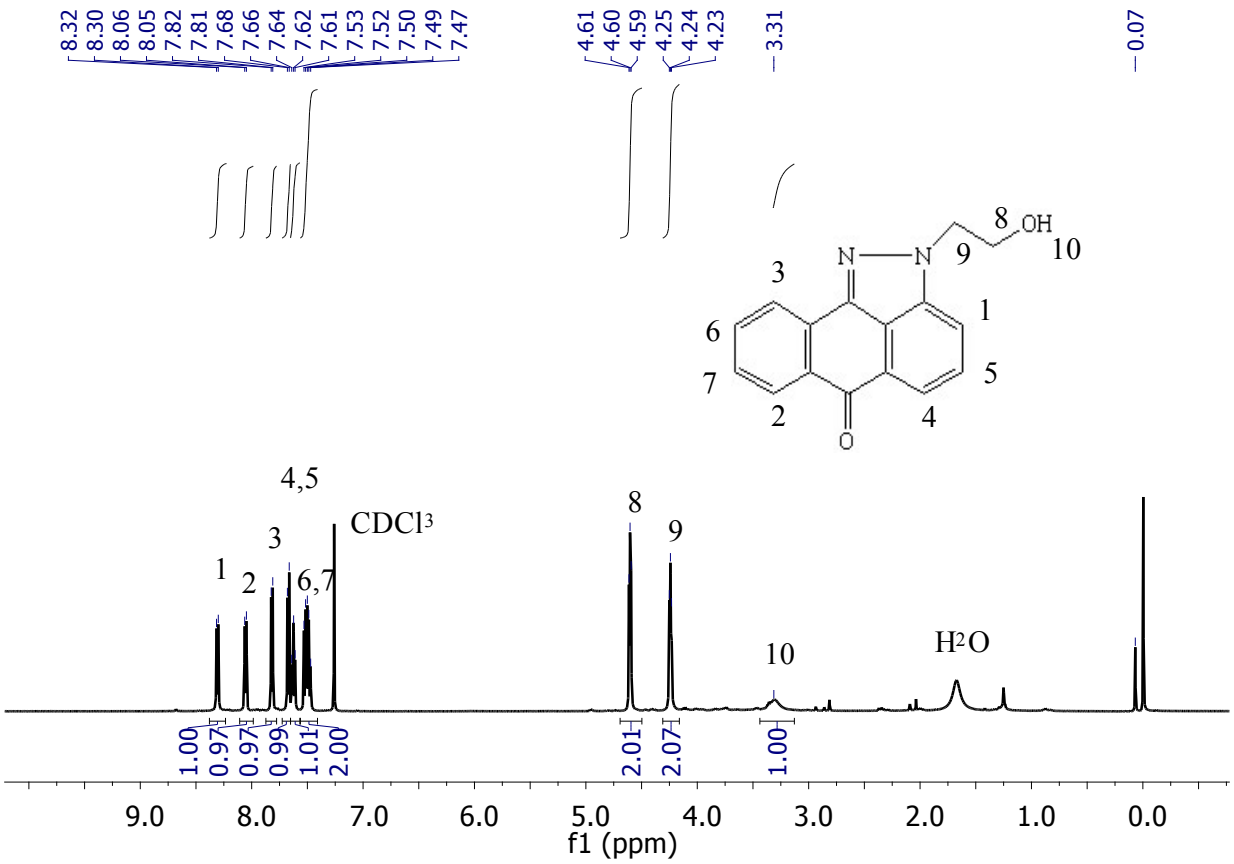

Fig. S1 ^{1}H NMR spectrum of SP-OH, measured in $CDCl_3$.

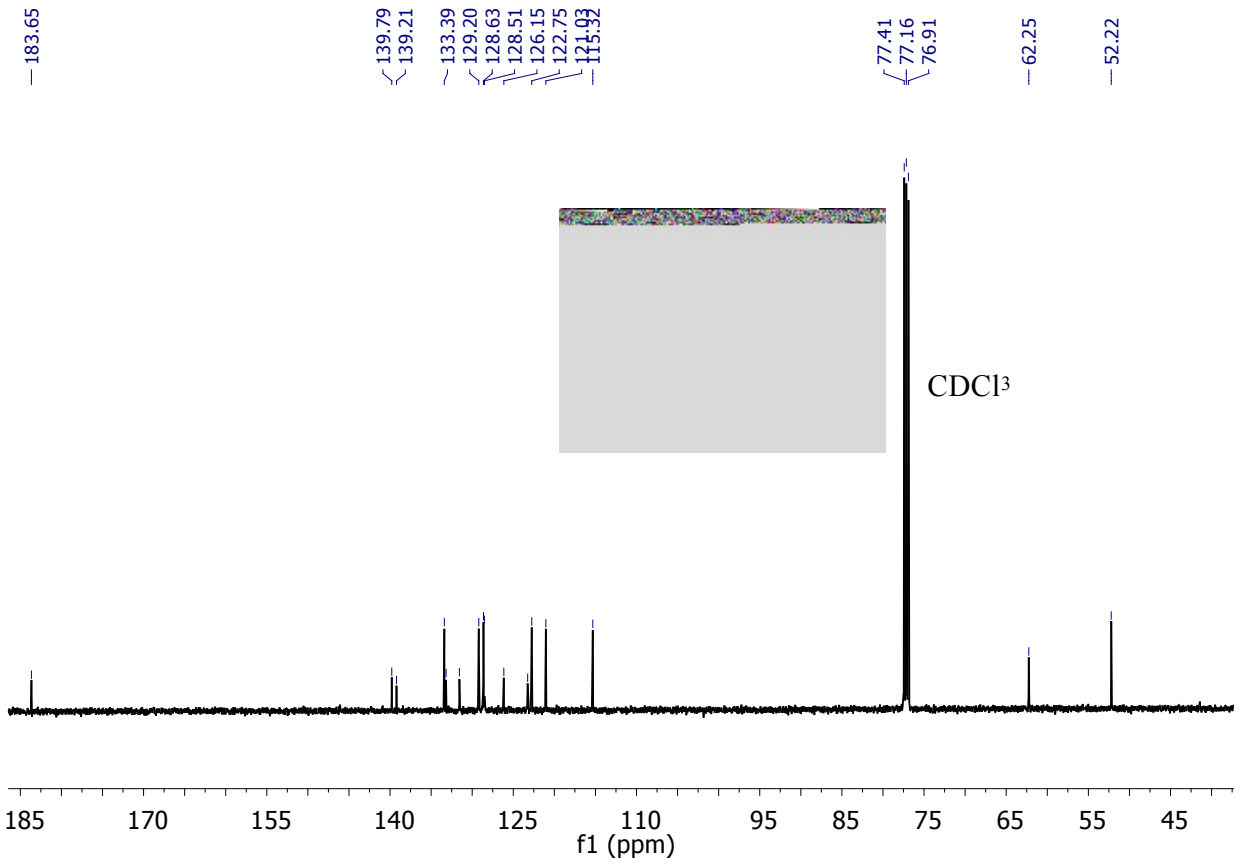

Fig. S2 ^{13}C NMR spectrum of SP-OH, measured in $CDCl_3$.

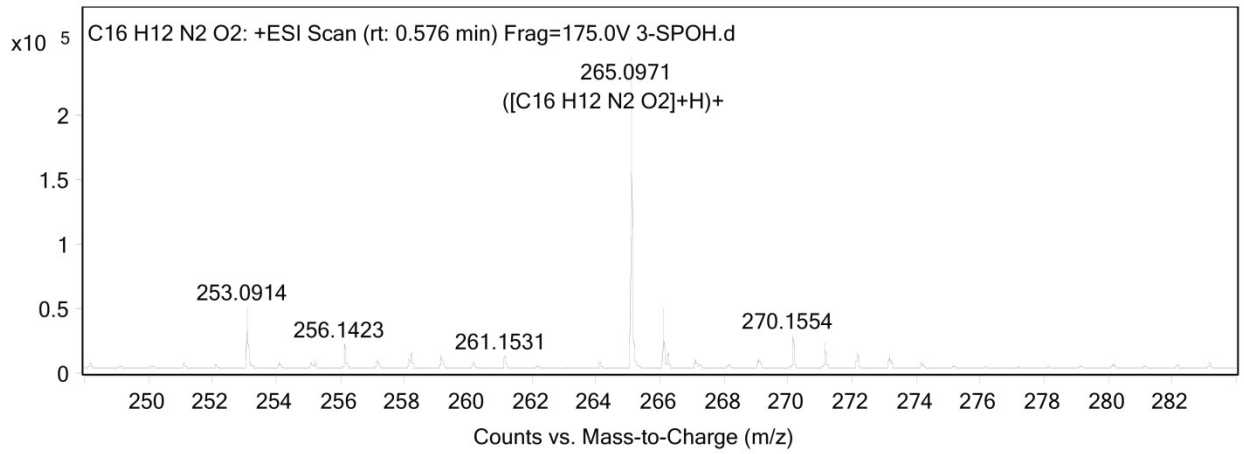

Fig. S3 ESI-MS spectrum of SP-OH

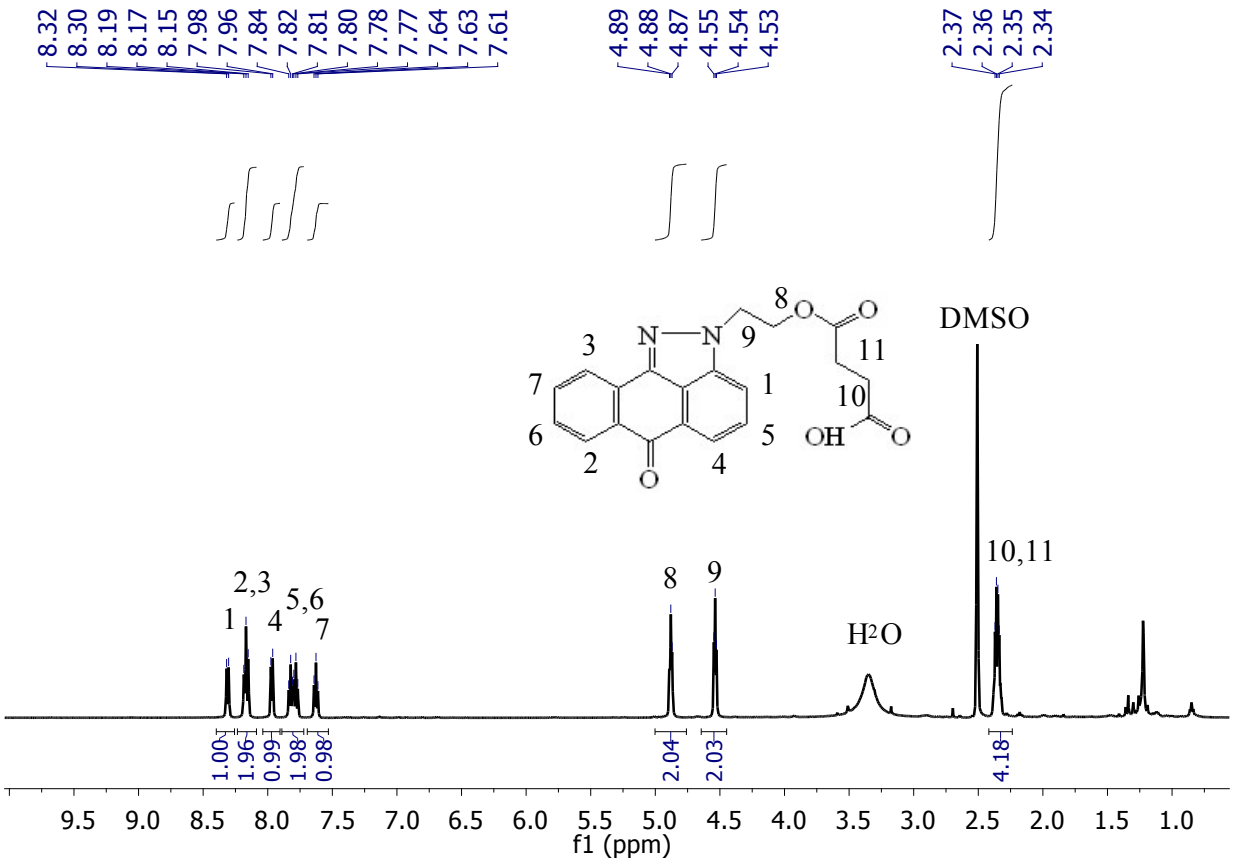

Fig. S4 ^{1}H NMR spectrum of SP-COOH, measured in DMSO-d_6.

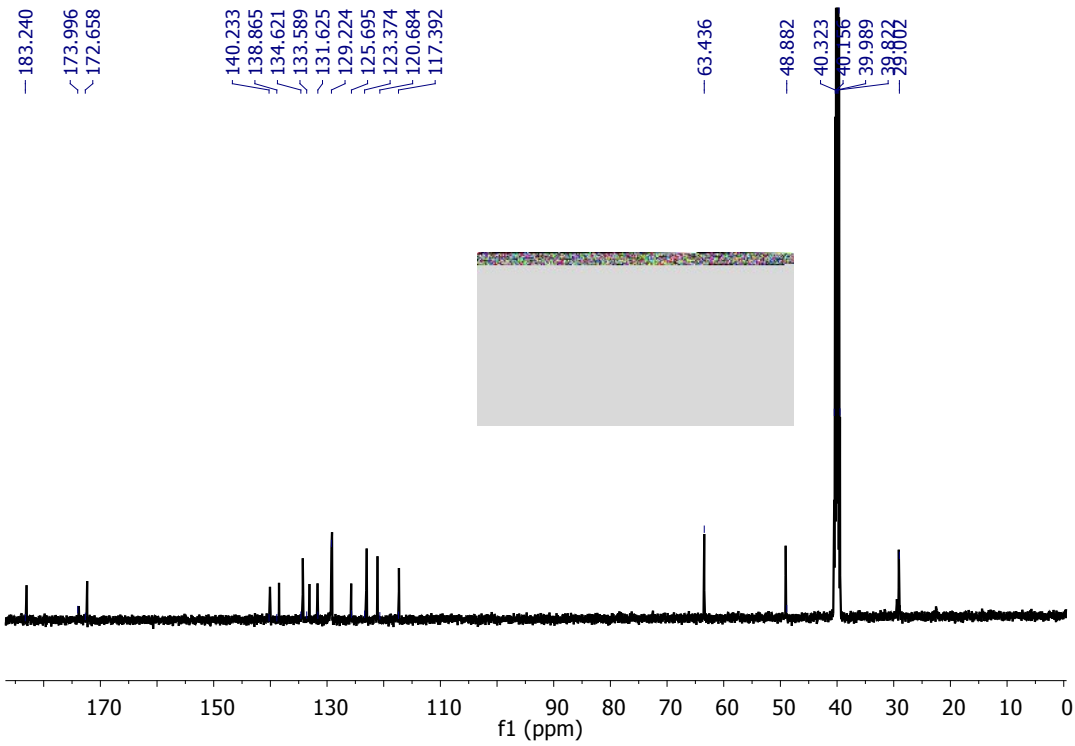

Fig. S5 ^{13}C NMR spectrum of SP-COOH, measured in DMSO-d_6.

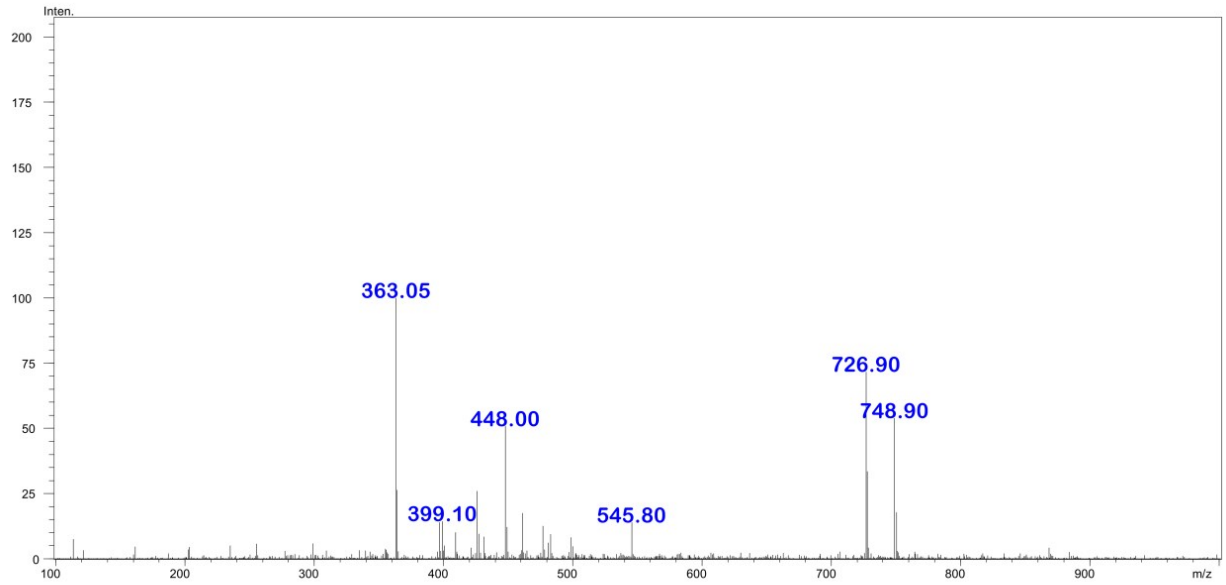

Fig. S6 LC-MS spectrum of SP-COOH

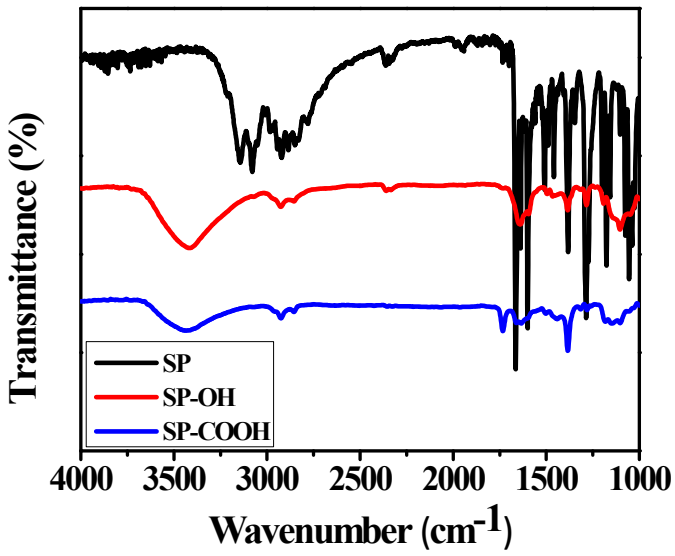

Fig. S7 IR spectra of SP, SP-OH and SP-COOH.

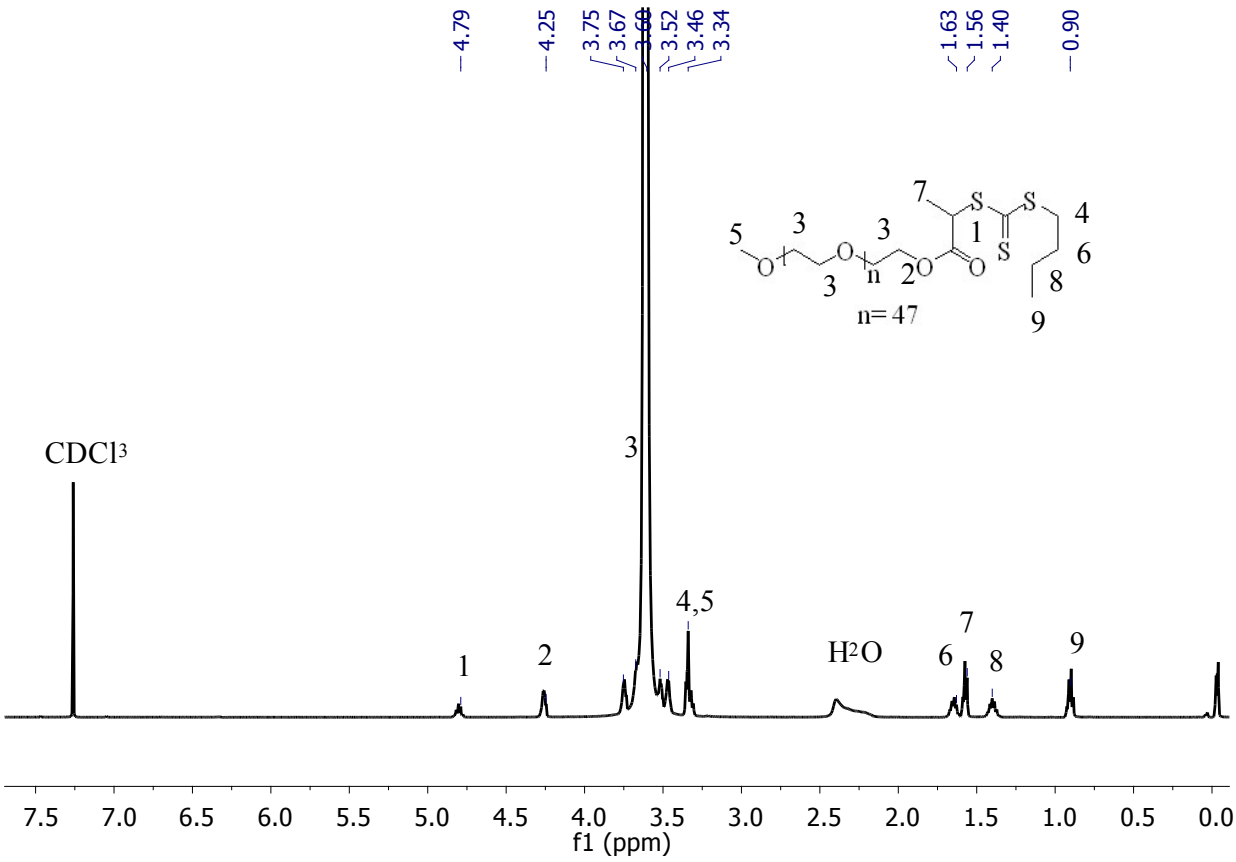

Fig. S8 ^{1}H NMR spectrum of $mPEG_{48}$ MacroCTA, measured in $CDCl_3$.

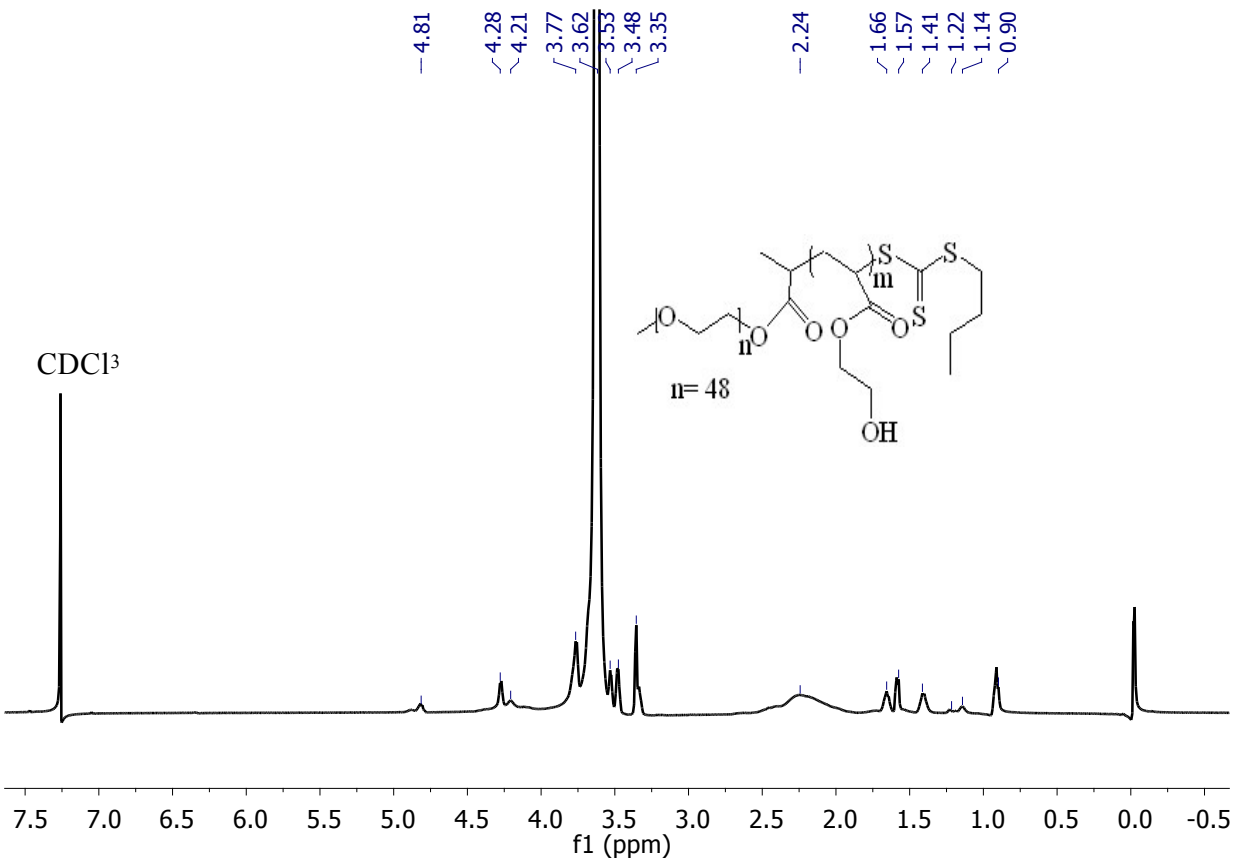

Fig. S9 ^{1}H NMR spectrum of mPEG$_{48}$-*b*-PHEA, measured in $CDCl_3$.

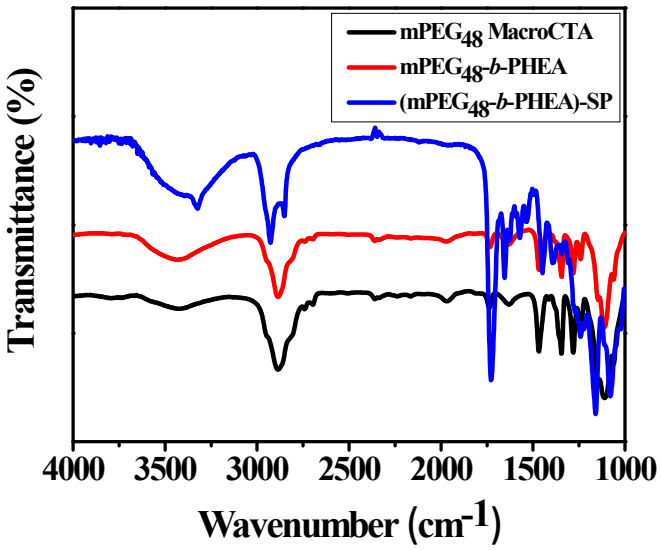

Fig. S10 FTIR spectra of polymers.

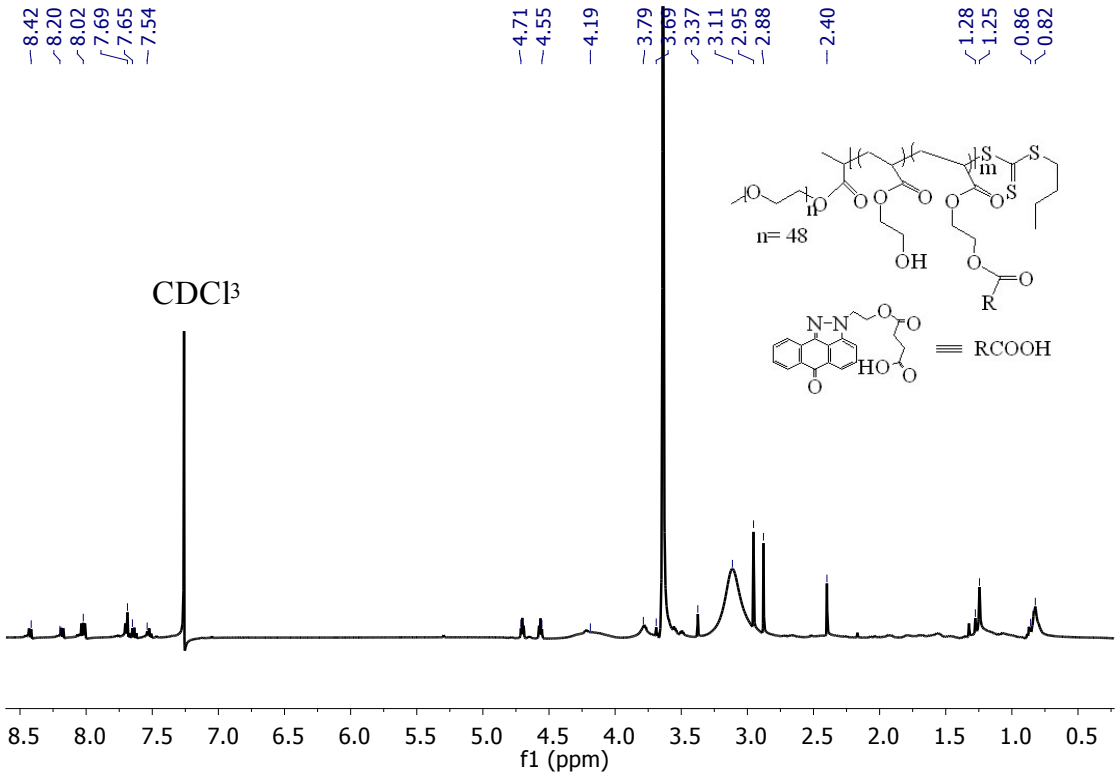

Fig. S11 ^{1}H NMR spectrum of (mPEG$_{48}$-*b*-PHEA)-SP, measured in $CDCl_3$.

2. SEC analysis

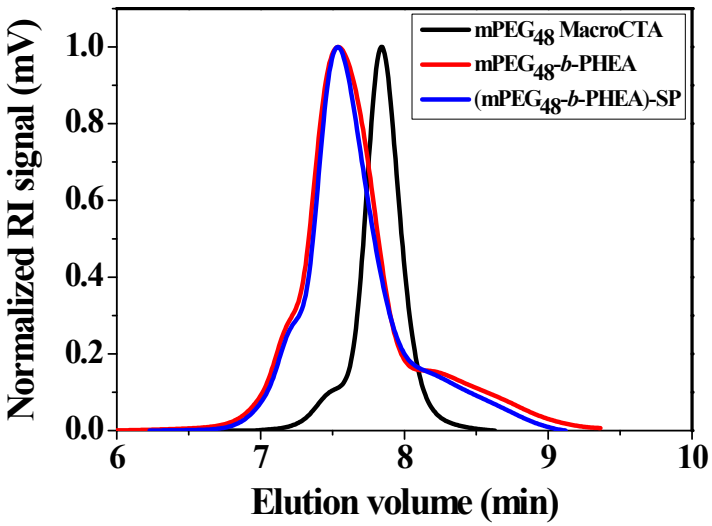

Fig. S12 GPC traces of polymers.

Table S1. Summary on the crystallographic data of SP-COOH.

Compound	**SP-COOH**
Formula	$C_{20}H_{16}N_2O_5$
Formula weight	364.35
Crystal system	orthorhombic
Space group	Pbca
a (Å)	7.7009(7)
b (Å)	18.4626(17)
c (Å)	24.055(3)
α (°)	90
β (°)	90
γ (°)	90
Volume (Å^3)	3420.1(6)
Z	8
Temperature (K)	293(2)
Density (g cm^{-3})	1.415
μ (mm^{-1})	0.103
F (000)	1520
$h_{min, max}$	-9, 8
$k_{min, max}$	-23, 23
$l_{min, max}$	-26, 31
No. of measured reflections	1330
No. of unique reflections	1570
No. of reflections used	3897
R_{all}, R_{obs}	0.1855, 0.0768
$wR2\_{all}$, $wR2\_{obs}$	0.215, 0.1528
$\Delta\rho_{min, max}$ (e Å^{-3})	-0.260, 0.321
GOOF	1.017

3. Computational studies (DFT)

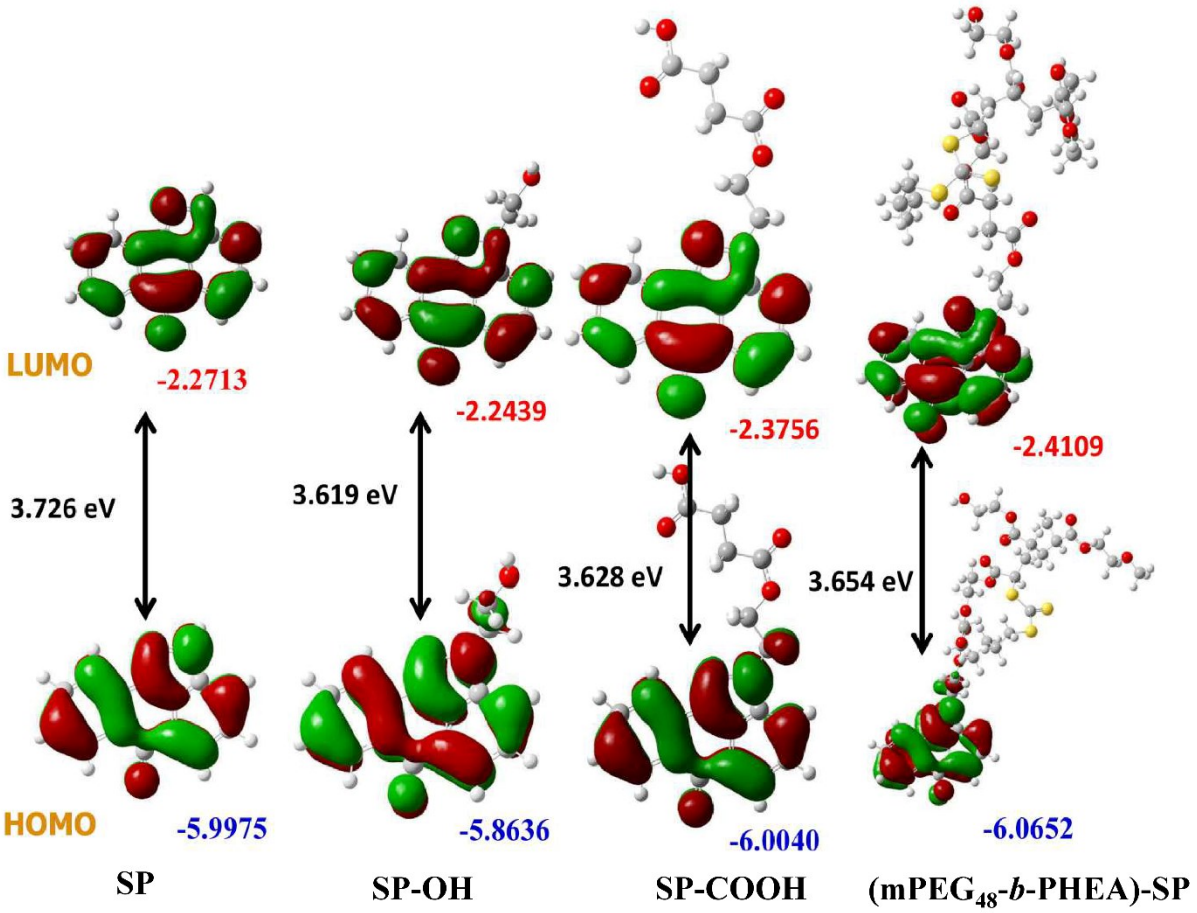

Fig. S13 Frontier molecular orbital electron density of SP, SP-OH, SP-COOH and (mPEG$_{48}$-*b*-PHEA)-SP.

4. Fluorescence studies

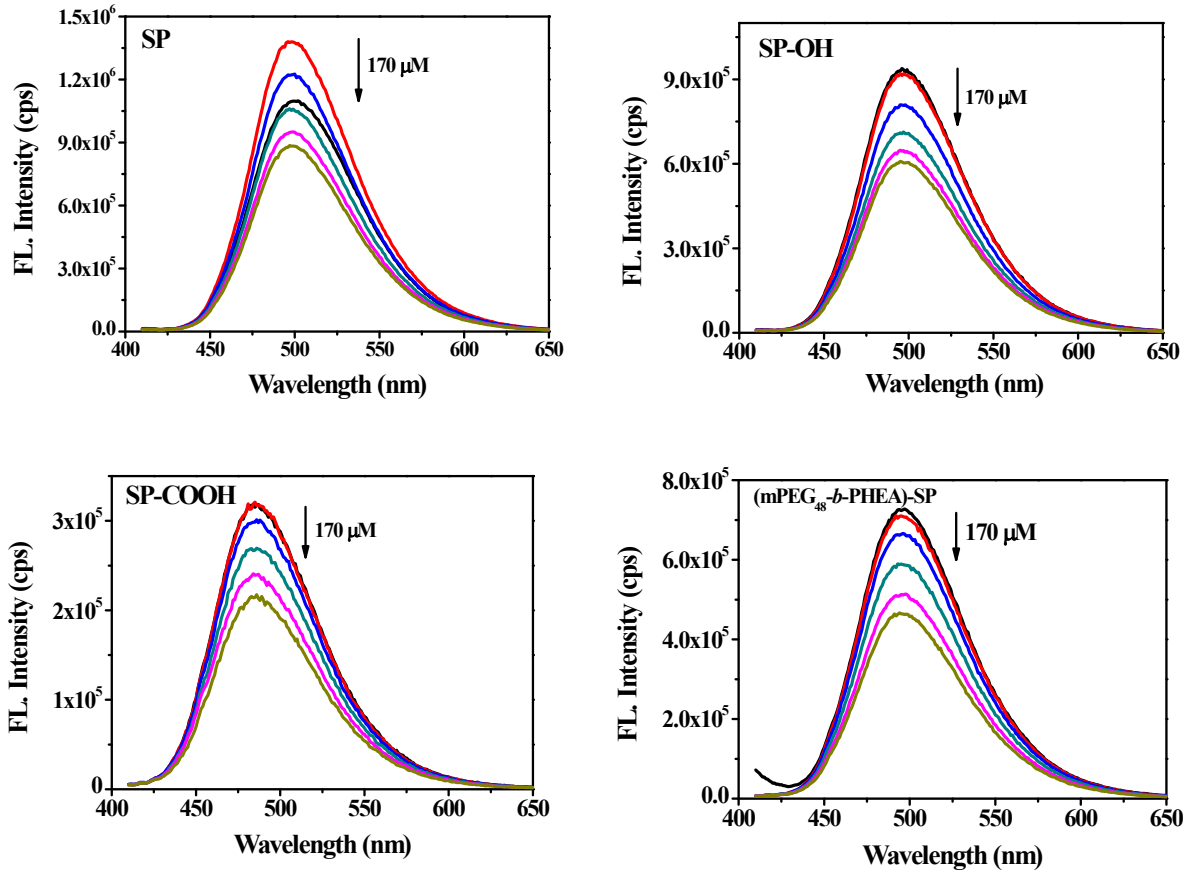

Fig. S14 Fluorescence quenching behaviour of SP derivatives and (mPEG$_{48}$-*b*-PHEA)-SP with NB.

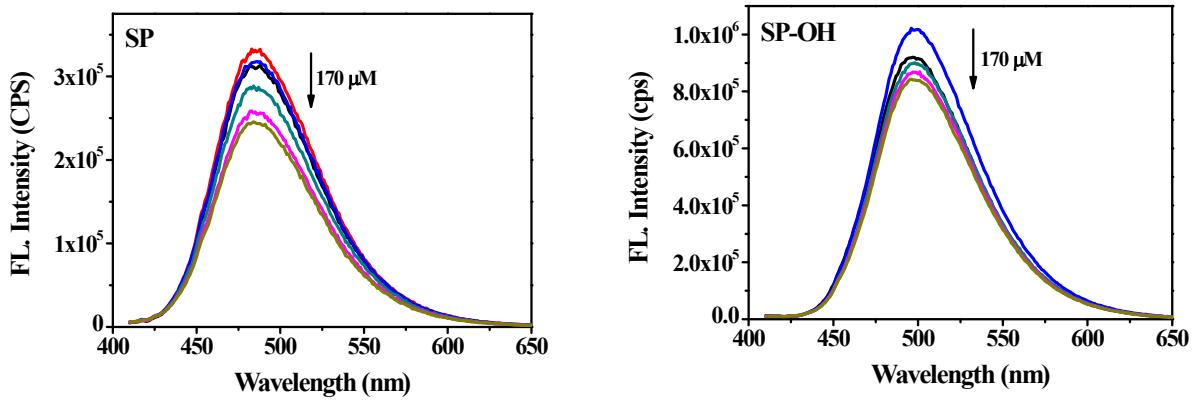

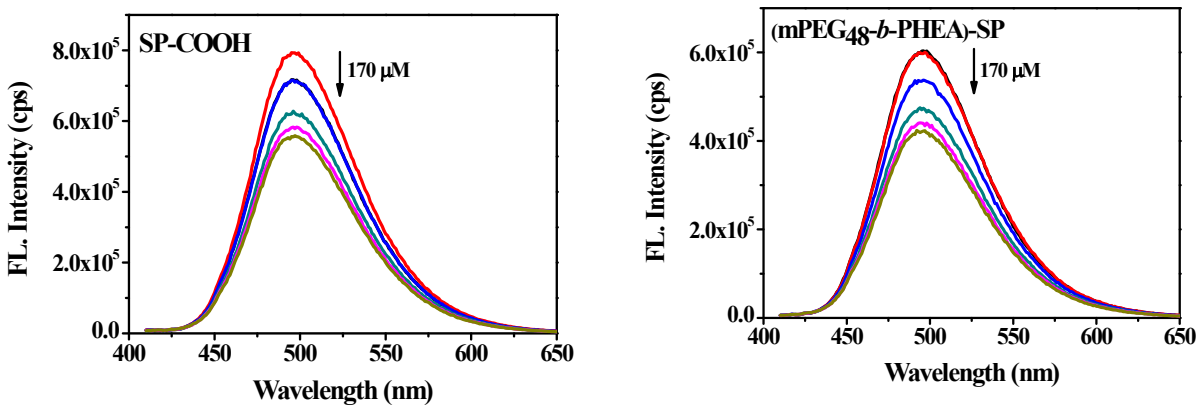

Fig. S15 Fluorescence quenching behaviour of SP derivatives and ($mPEG_{48}$-*b*-PHEA)-SP with NT.

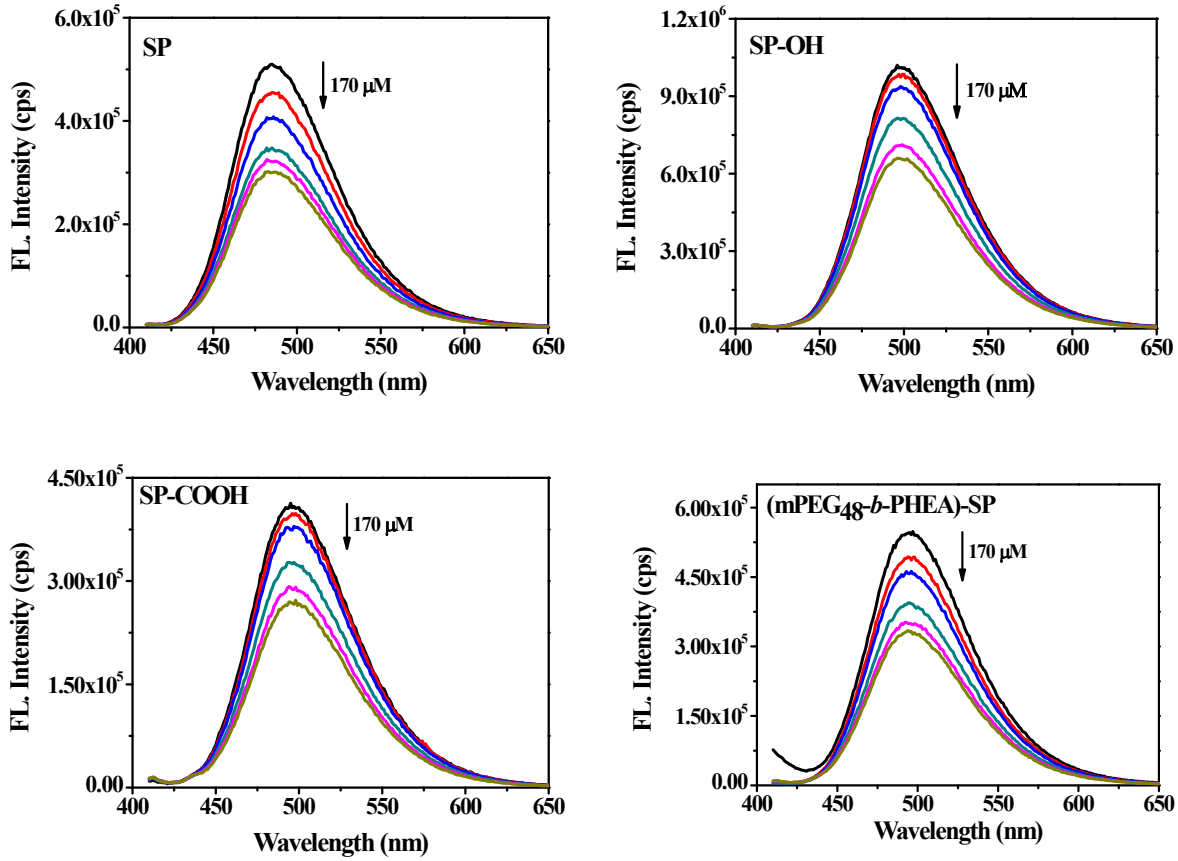

Fig. S16 Fluorescence quenching behaviour of SP derivatives and ($mPEG_{48}$-*b*-PHEA)-SP with NP.

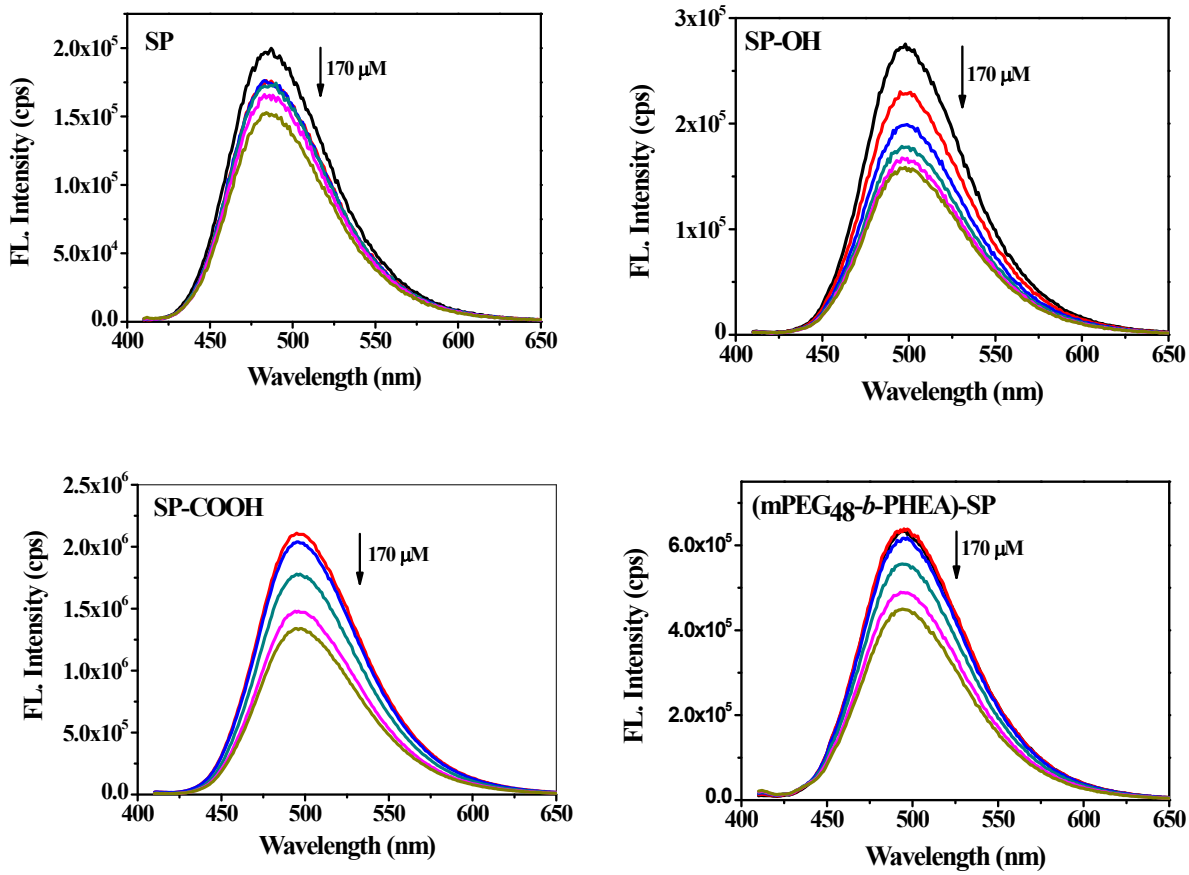

Fig. S17 Fluorescence quenching behaviour of SP derivatives and ($mPEG_{48}$-*b*-PHEA)-SP with DNP.

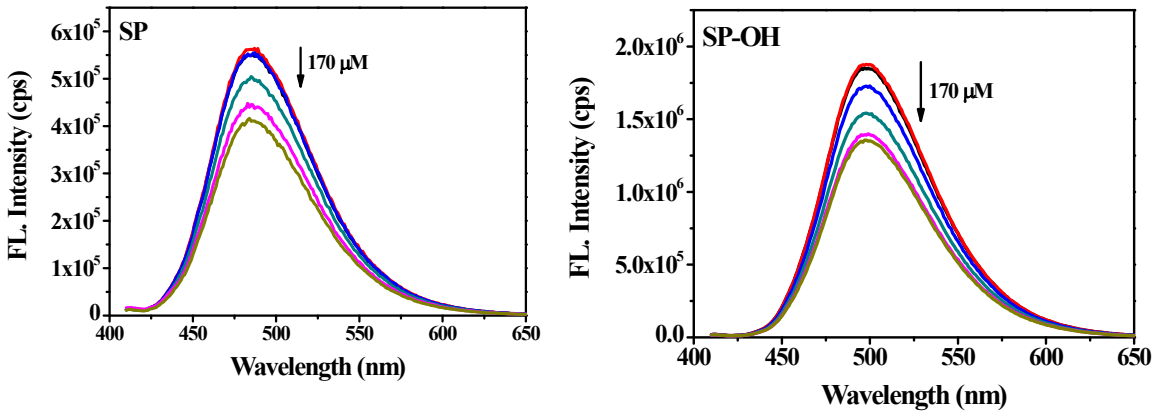

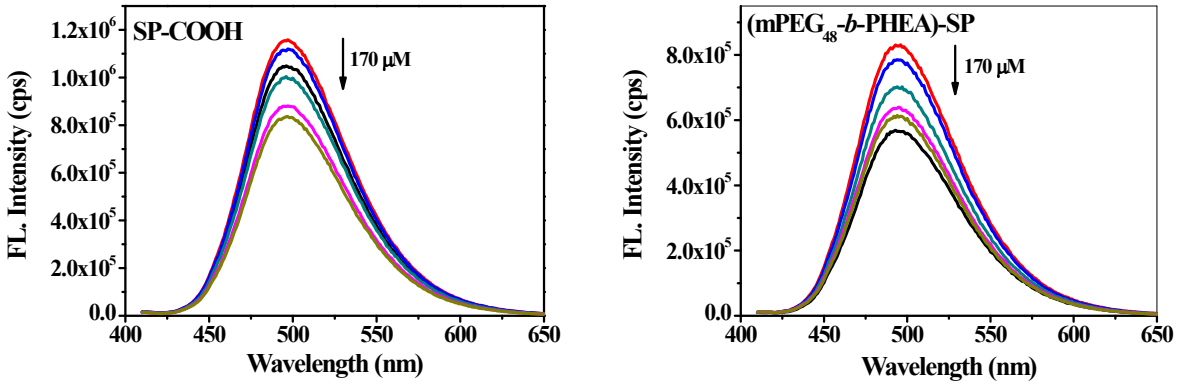

Fig. S18 Fluorescence quenching behaviour of SP derivatives and (mPEG$_{48}$-*b*-PHEA)-SP with H_2O_2.

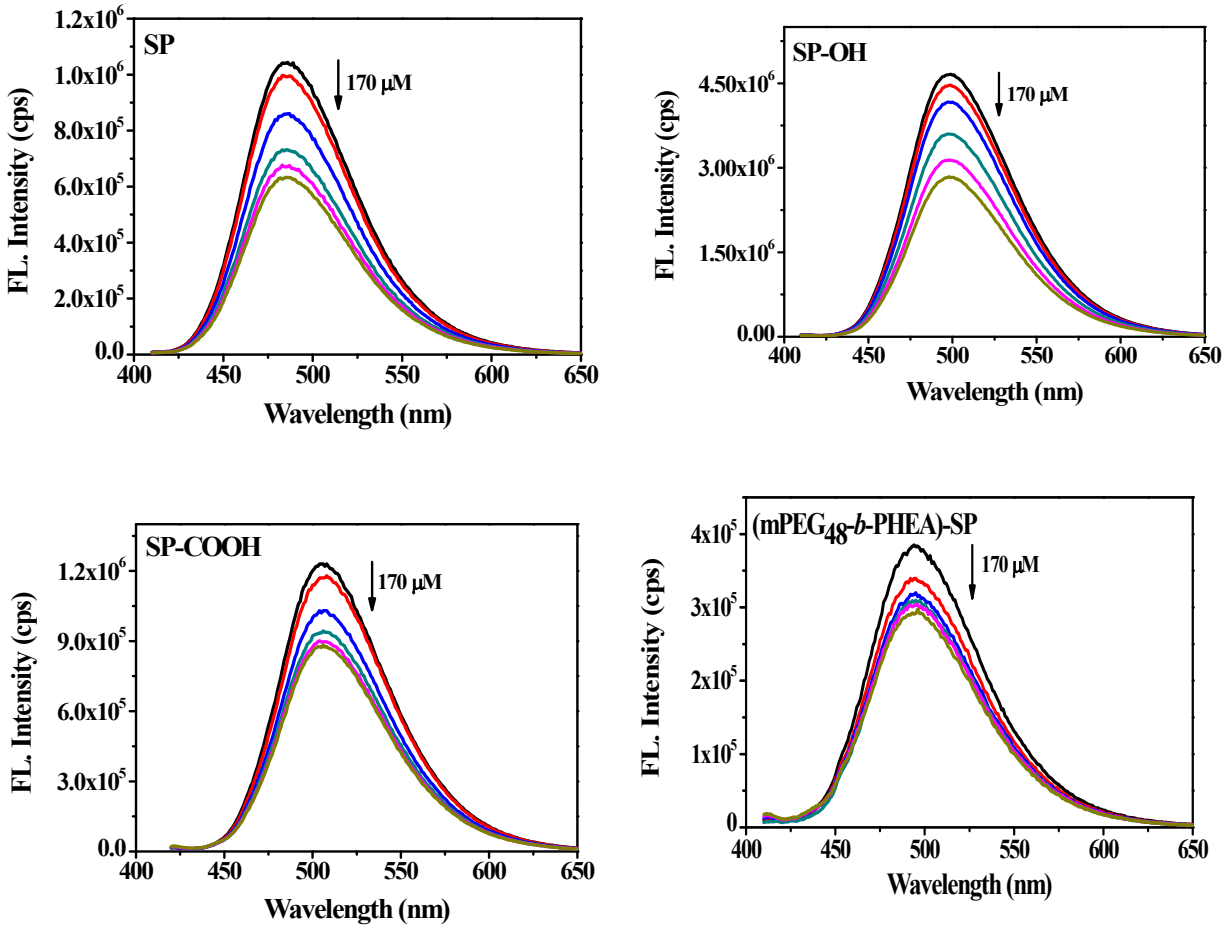

Fig. S19 Fluorescence quenching behaviour of SP derivatives and (mPEG$_{48}$-*b*-PHEA)-SP with Metronidazole.

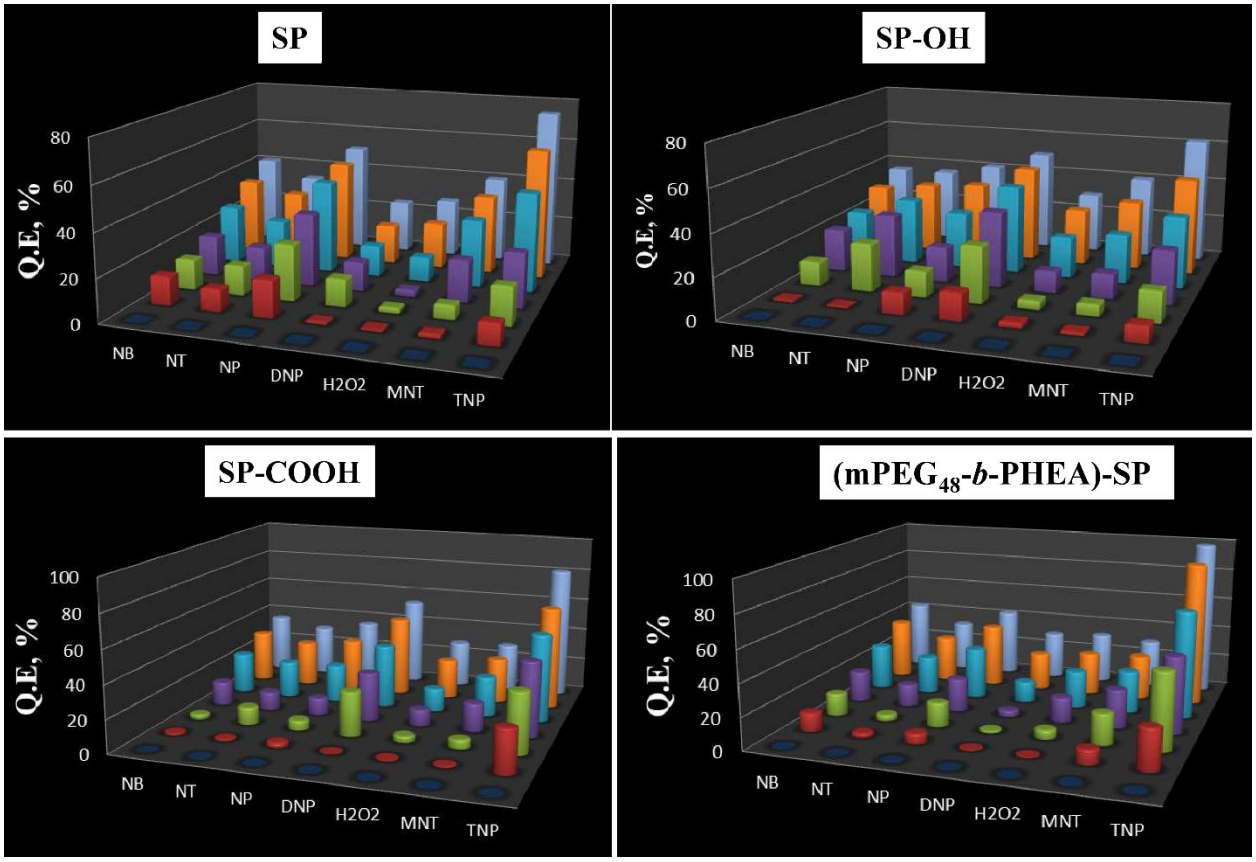

Fig. S20 Comparison in the quenching efficiency of SP derivatives and (mPEG$_{48}$-*b*-PHEA)-SP with different nitro analytes and nitro antibiotics (0-170 μM).

5. Stern-Volmer Rate constants

Table S2 Summary on the calculated Ksv values (M^{-1}) of different SP derivatives and block (co)polymer with different nitroanalytes and nitroantibiotics.

Compound	NB	NT	NP	DNP	TNP	H_2O_2	Metronidazole
SP	3237	2477	5482	2512	2.61×10^4	1468	3313
SP-OH	2548	3024	2990	4901	5.0×10^4	1765	2548
SP-COOH	2152	2595	5138	5487	6.91×10^4	1722	2159
(mPEG$_{48}$-*b*-PHEA)-SP	3512	2297	3713	5986	9.74×10^4	2226	2499

6. Determination of Limit of Detection (LODs):

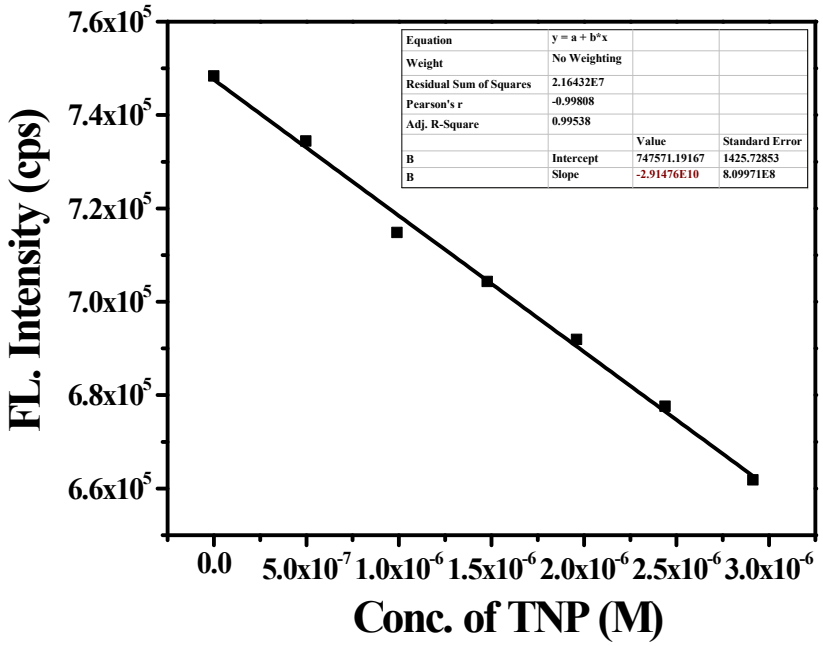

Fig. S21 Change in the emission intensity of (mPEG$_{48}$-*b*-PHEA)-SP at 496 nm for different concentrations of TNP.

7. UV-Visible titration study of co-poylmer and NACs

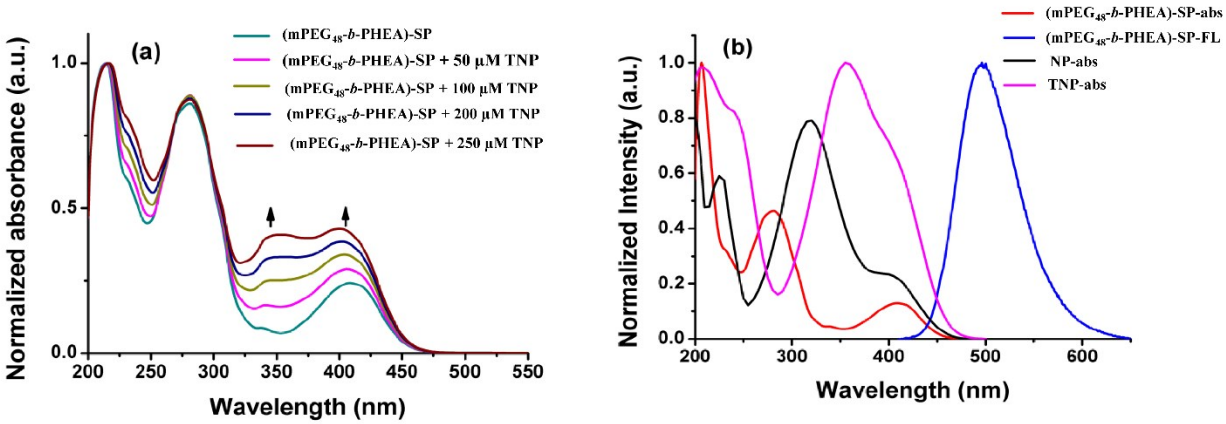

Fig. S22 (a) Change in the absorption spectra of (mPEG$_{48}$-*b*-PHEA)-SP (30 x 10^{-6} M) upon addition of different concentrations of TNP. (b) Normalized UV-Vis spectrum of 4-nitro phenol and TNP compounds overlapping with normalized emission spectra of (mPEG$_{48}$-*b*-PHEA)-SP in methanol.

8. UV-Visible titration study with TNP and other acids

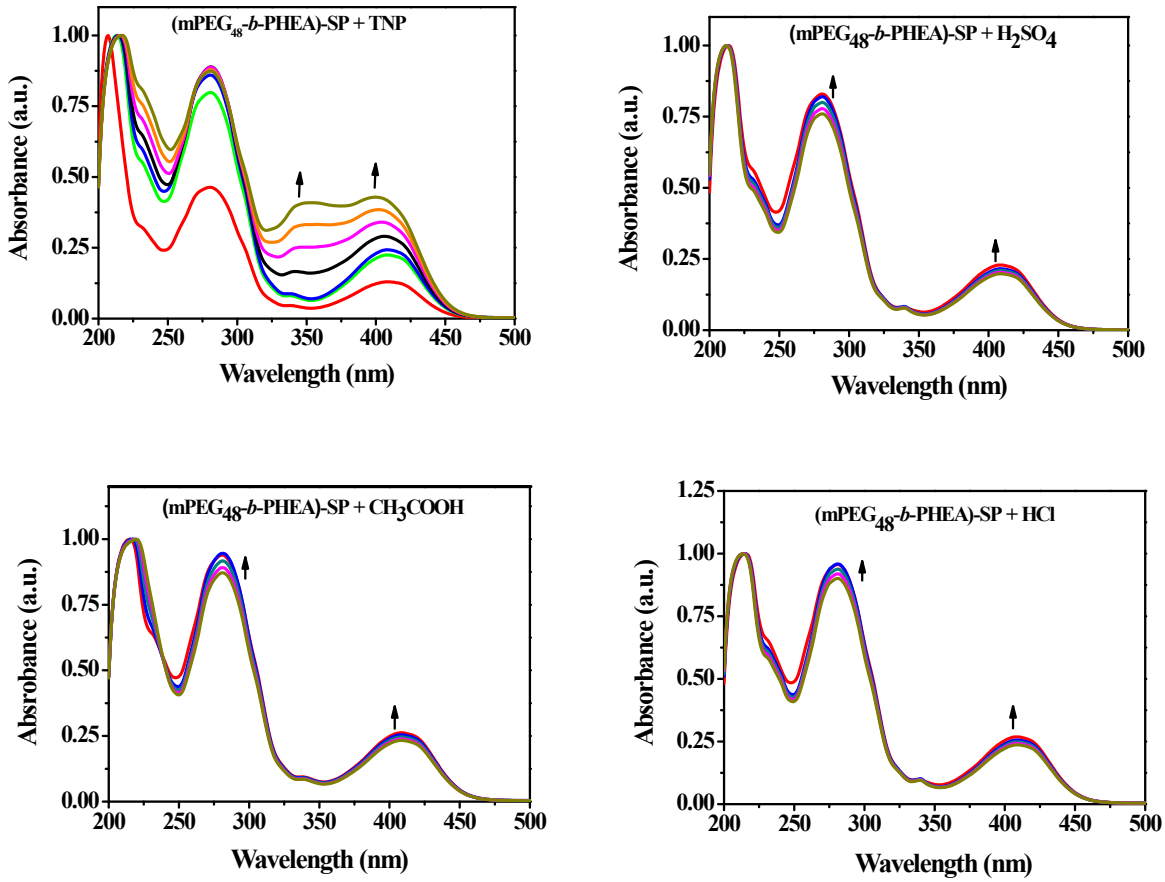

Fig. S23 Variation in the absorption spectra of (mPEG$_{48}$-*b*-PHEA)-SP upon addition of different concentrations of TNP, H_2SO_4, acetic acid and HCl.

9. Fluorescence lifetime decay of co-polymer with TNP

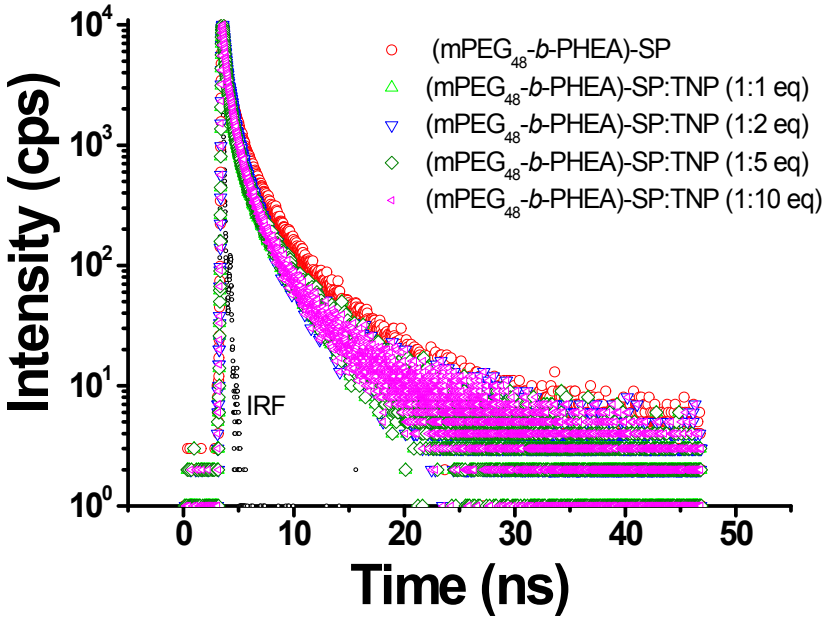

Fig. S24 Change in the fluorescence decay of ($mPEG_{48}$-*b*-PHEA)-SP ($5x10^{-6}$ M) in methanol and treated with different concentration of TNP at λ_{em}= 500 nm.